

Design and Modal Analysis of End-Winding Support Systems in Induction Motors

Behzad Bahrami Joo^a, Mohsen Nikfar^{b*}

^a *Mechanical Design Specialist, R&D Department, MAPNA Generator Engineering and Manufacturing (PARS), Karaj, Iran; Bahramijoo@pars.mapnagroup.com.*

^b *Head of Mechanical Design Group, R&D Department, MAPNA Generator Engineering and Manufacturing (PARS), Karaj, Iran; Nikfar@pars.mapnagroup.com.*

* *Corresponding author e-mail: Nikfar@pars.mapnagroup.com*

Abstract

The design of an electric motor must account for multiple structural requirements to ensure sufficient resistance against operational stresses and prevent premature failures. Among these considerations, frequency analysis of different components plays a critical role in evaluating their dynamic behaviour. This study investigates the modal characteristics of the end-winding region of a medium-power, four-pole induction motor. Due to the machine configuration, the dominant structural response under excitation corresponds to an eighth nodal diameter mode shape. To enhance vibration resistance, various supporting system designs were developed and analysed using modal analysis. Several alternatives were proposed based on the number of roping rows and the placement of aluminium support rings. Comparative frequency analysis revealed that using an aluminium annular ring roped around the coils significantly improves system stiffness and raises natural frequencies. The location of this ring was found to be a critical parameter, with positioning near the coil bends yielding superior results. Based on the results, the best-designed model demonstrated the highest natural frequencies and was identified as the most effective configuration.

Keywords: Induction motor, end-winding, modal analysis, natural frequency

1. Introduction

In electrical machines, resonance occurs when the natural and excitation frequencies coincide, leading to critical vibration levels. In two-pole machines, a 50 Hz rotational speed produces an ef-

fective 100 Hz electromagnetic excitation due to the twice-per-revolution magnetic force component. Similarly, in four-pole machines operating at 1500 rpm, the mechanical frequency is 25 Hz, while the dominant electromagnetic excitation still occurs at 100 Hz. Therefore, the natural frequencies of the four-node (two-pole) and eight-node (four-pole) vibration modes must be adequately separated from the 100 Hz excitation frequency. Typically, the end-winding natural frequencies exceed 100 Hz owing to their structural stiffness and material characteristics, which ensures stable vibration behaviour. Moreover, electrical machines designed with more than four poles exhibit excitation patterns associated with higher-order circumferential mode shapes. Consequently, the natural frequencies of the end-winding region in these configurations are generally well separated from the 100 Hz excitation, and such machines rarely encounter resonance issues in frequency-domain analyses. Nevertheless, once the vibrational response of the end-winding region is verified to be satisfactory, stress analysis under critical loading conditions should also be performed to ensure mechanical robustness. It should also be noted that, due to their simpler structural layout, more flexible coils, and smaller overall dimensions compared with large generators, electrical motors tend to exhibit a more pronounced decrease in natural frequencies under operational conditions. For this reason, manufacturers emphasize maintaining a sufficient margin between the structural natural frequencies and the excitation frequencies to prevent resonance.

Previous studies have extensively analysed the vibration behaviour of electrical machine stator end-windings to improve reliability and design. Finite element methods have been widely used to determine electromagnetic forces and natural frequencies [1, 2], while operational vibration data analysis has been applied to extract modal characteristics under real operating conditions [3]. Several works emphasize the importance of vibration monitoring in high-speed machines to prevent end-winding failures [4]. Experimental investigations, such as those by Kumar et al. [5], have demonstrated that modal testing and structural reinforcement can effectively reduce resonance-induced vibrations in large generators. More recently, Zhao et al. [6] introduced a response surface approach to model the dynamic behaviour of stator end-windings, enabling efficient prediction and optimization of natural frequencies and vibration modes. Samadpour et al. [7] analysed a 250 MVA MAPNA turbogenerator, introducing a novel support system that effectively mitigates resonance and short-circuit-induced vibrations, validated through both FEM and experiments. Other research has employed experimental modal analysis to detect mechanical looseness in induction machine end-windings [8], enhancing diagnostic and maintenance accuracy. Additionally, a new analytical method has been proposed to calculate the natural frequencies of radial-flux slotted motors while accounting for end cover effects [9], enabling more precise vibration and noise predictions. In another study [10], the authors conducted a multiphysics FEM study on the stator end-winding support system of a medium-power turbogenerator, highlighting the role of optimized support design in reducing vibration and enhancing durability. Similarly, Shahparasti et al. [11] employed modal and harmonic analyses to refine frame and stator core structures, demonstrating how design modifications mitigate resonance and improve dynamic stability.

In this study, the end-winding system of a medium-power induction motor, fully designed and developed at MAPNA Pars Generator, is analysed in the frequency domain, and an appropriate supporting system is proposed to control its vibrations.

2. Problem Definition and Objectives

The stator end-winding region in electrical machines is highly susceptible to mechanical and thermal stresses arising from electromagnetic forces, temperature gradients, and vibrations, particularly in machines with long end-windings. To maintain structural integrity and minimize vibration, end-winding support systems are employed, ranging from simple roping in low-power motors to complex assemblies of brackets, composite support rings, and wedges in large generators. In this study, a detailed finite element model was developed in ANSYS 2020 to investigate the frequency response of the end-winding region. The analysis ensures accurate prediction of vibrational behav-

our and supports the assessment of structural reliability and durability. Unlike previous studies that primarily focus on general end-winding dynamics, this work provides a systematic, design-oriented investigation of practical end-winding support configurations under realistic industrial constraints. The study emphasizes the relative influence of roping layout and support ring position on the critical eight-node mode, which is of particular importance for four-pole induction machines.

3. Initiating the Model

After 3D modeling of a turbo-generator in CAD software, a series of modifications must be implemented to prepare the model for subsequent analysis.

3.1 Material Specifications

One of the most important considerations is to assign the correct material specification to the different parts so that the designed CAD model is similar to the real one in terms of vibration and modal behavior. It is worth noting that the material specification of some parts such as bars and roping system, which are complex components, can only be extracted through modal testing. Furthermore, additional material components, such as spacer or resin mat, are derived from previous research and standards. With all these considerations, some of the notable material specifications of parts are shown in Table 1.

Table 1. Induction Motor Material Specifications

Components	Material Name	Young's Modulus (GPa)	Density (kg/m ³)
Coils	-	73.9	6342
Resin Mat	-	0.425	2000
Roping	-	0.120	2000
Stator Core	Laminated Layers	185 (Radial) 1.55 (Axial)	6041

3.2 Geometry consideration

In the vibration analysis of an induction motor, accurate preparation of the three-dimensional model for finite element analysis is of great importance. The CAD model must be simplified as much as possible for efficient simulation, while maintaining close structural similarity to the actual analytical model. Fig. 1 illustrates the stator of a medium-power induction motor manufactured by MAPNA Pars Generator. The model includes the equivalent stator core, press plate, tension bar, and the end-winding region of the coils.

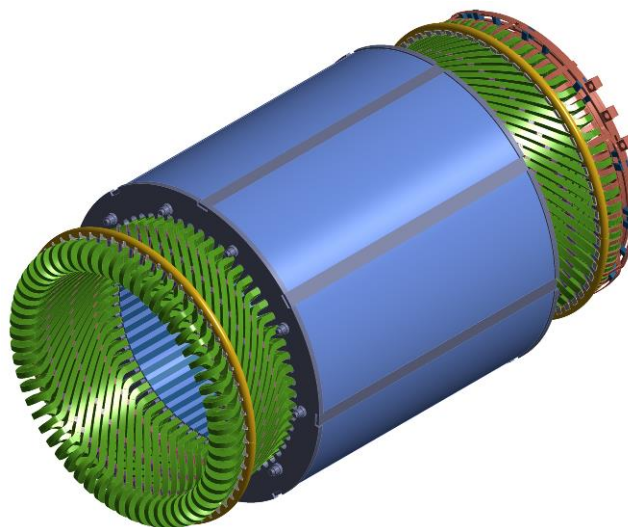


Figure 1. Stator model used in finite element analysis

4. Methods

The methodology was designed to enable a direct and consistent comparison between different end-winding support configurations. To isolate the influence of each design parameter, all analyses were conducted using the same geometric model, material definitions, and boundary conditions, with only the support system layout being modified between cases.

Following the preparation of the three-dimensional stator model, a linear modal analysis was performed to extract the natural frequencies and corresponding mode shapes of the end-winding region. In four-pole induction machines, particular attention was given to the eight-node mode shape, as this mode is known to be critical with respect to electromagnetic excitation and resonance avoidance [12]. For each support configuration, the natural frequency of this mode was identified and used as the primary metric for comparison. The objective was to assess the relative effectiveness of different support layouts in increasing structural stiffness and reducing vibration susceptibility in the end-winding system.

4.1 Finite Element Modelling Details

The finite element model was developed in ANSYS using a three-dimensional solid formulation. SOLID186 and SOLID187 elements were employed to accurately represent both regular regions and geometrically complex parts of the stator and end-winding assemblies. Mesh refinement was applied primarily in the end-winding region and in the supporting components, where higher deformation gradients were expected to influence the modal response.

Mechanical connections between components were modeled as bonded contacts using the Multi-Point Constraint (MPC) formulation. Mesh convergence was verified by progressively refining the mesh until changes in the extracted natural frequencies became negligible. The final mesh density was selected as a compromise between numerical accuracy and computational efficiency.

4.2 Model Validation and Industrial Background

The investigated induction motor is currently in the design phase, and experimental modal testing on the final product is therefore not yet available. Nevertheless, the modeling strategy, material properties, and end-winding support concepts adopted in this study are grounded in prior industrial experience and validated test data from previously manufactured and tested induction motors and generators of comparable size and power rating. These existing designs and measurements were used as practical reference points to guide the numerical modeling and to ensure that the simulated configurations remain representative of realistic industrial practice.

5. Analysis Results

This section presents the results of the modal analysis of the induction motor end-winding region for different support system designs. Five different configurations were evaluated, and among these models, one was identified as the optimal design for implementation in the motor's end-winding region.

5.1 The Type A design: 3-Rows of roping and a central aluminium ring

In the initial and baseline design of the end-winding support system, three rows of roping with spacers were used in the end region. Additionally, the entire end-winding region was restrained at its midsection by an aluminum ring with a diameter of 15 mm. The corresponding model is shown in Fig. 2.

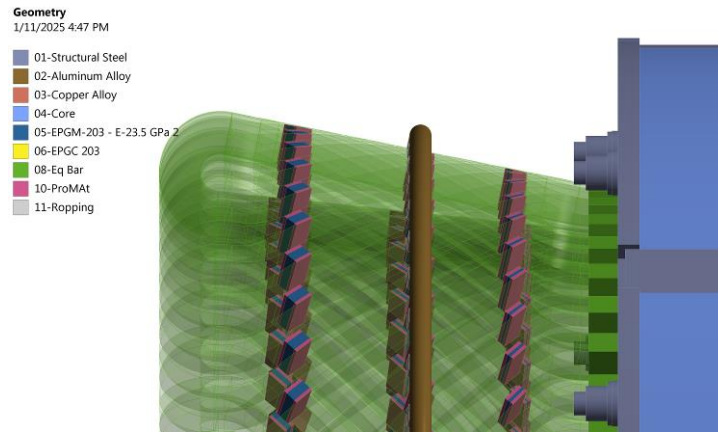


Figure 2. End-winding support system; Type A.

In this preliminary support system design, the Young’s modulus of the roping connecting the aluminum ring to the coils was analyzed with two values: 120 MPa (based on the previous analysis conducted in MAPNA Pars Generator) and a higher value of 200 MPa. In a separate analysis, the aluminum ring was removed from the support assembly to assess its effect on the natural frequencies of the end-winding region. According to Table 2, with a roping Young’s modulus of 120 MPa, the eight-node natural frequency of the induction motor end-winding is calculated as 234.4 Hz.

Increasing the roping modulus to 200 MPa results in a natural frequency of 236.2 Hz, indicating that variations in roping properties have only a minor effect on the natural frequencies in this design.

Table 2. The Type A Design Frequency Response

Ring Roping Young’s Modulus (MPa)	With Ring		Without Ring
	E=120	E=200	
Mode Shape 4-Node (Hz)	163.39	166.49	158.86
Mode Shape 6-Node (Hz)	195.95	197.7	190.85
Mode Shape 8-Node (Hz)	234.43	236.2	229.5

5.2 The Type B design: 2-Rows of roping and an aluminium ring close to the press plate

After obtaining the results from the modal analysis of the end-winding region, the number of roping rows was reduced from three to two to simplify the manufacturing process and reduce material consumption, and the modal analysis was repeated. In this design, the coil end-roping at its original positions remains fixed, and instead of the first and middle rows, only a single roping row is introduced between them, as shown in Fig. 3. In this proposed configuration, the aluminum ring is also relocated to the position of the new roping row.

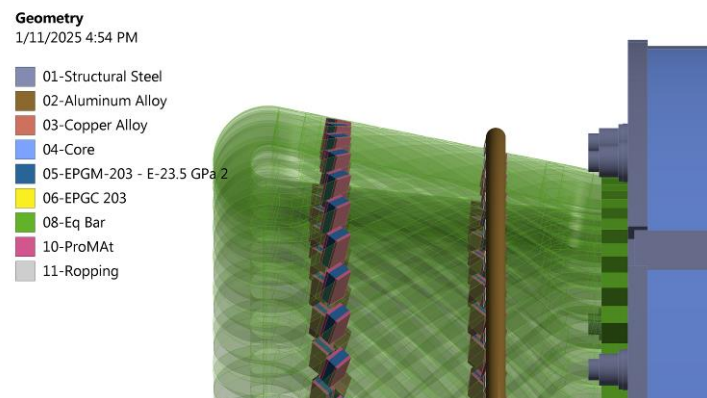


Figure 3. End-winding support system; Type B.

According to Table 3, for a roping Young’s modulus of 200 MPa, the natural frequency decreases by 12.4 Hz compared to Design A, reaching 223.8 Hz. This illustrates the significant impact that removing one roping row can have on the natural frequencies in this design.

Table 3. The Type B Design Frequency Response

Ring Roping Young’s Modulus (MPa)	With Ring		Without Ring
	E=120	E=200	
Mode Shape 4-Node (Hz)	153.05	153.72	150.22
Mode Shape 6-Node (Hz)	184.95	185.72	182.37
Mode Shape 8-Node (Hz)	222.95	223.8	220.4

5.3 The Type C design: 2-Rows of roping and an aluminium ring away from the press plate

In this section, a further modification is applied to Type B. In the Type C design, while keeping the location and number of roping rows unchanged, the aluminum ring is relocated to the end of the coil (Fig. 4). In the results from Types A and B, it was observed that the aluminum ring at the previously proposed positions had little effect on the natural frequencies of the end-winding region.

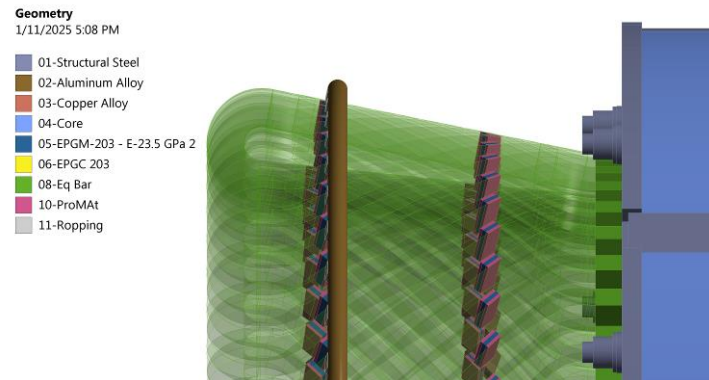


Figure 4. End-winding support system; Type C.

After relocating the aluminum ring to the new position, the eight-node natural frequency of the support system with a roping Young’s modulus of 200 MPa increases by 16.7 Hz, reaching 240.5 Hz. This demonstrates the substantial influence that the distance of the ring from the press plate can have on the natural frequencies.

Table 4. The Type C Design Frequency Response

Ring Roping Young’s Modulus (MPa)	With Ring		Without Ring
	E=120	E=200	
Mode Shape 4-Node (Hz)	172.9	175.69	150.22
Mode Shape 6-Node (Hz)	199.47	204.3	182.37
Mode Shape 8-Node (Hz)	235.6	240.46	220.4

5.4 The Type D design: 3-Rows of roping and an aluminium ring away from the press plate

In the fourth support system design, the new position of the aluminum ring is retained due to its significant effect on increasing the natural frequencies, while the roping configuration is reverted to Design A (Fig. 5). After implementing these changes, it is observed that the eight-node natural frequency with a roping Young’s modulus of 200 MPa reaches 248.3 Hz, representing an increase of nearly 8 Hz compared to the previous configuration.

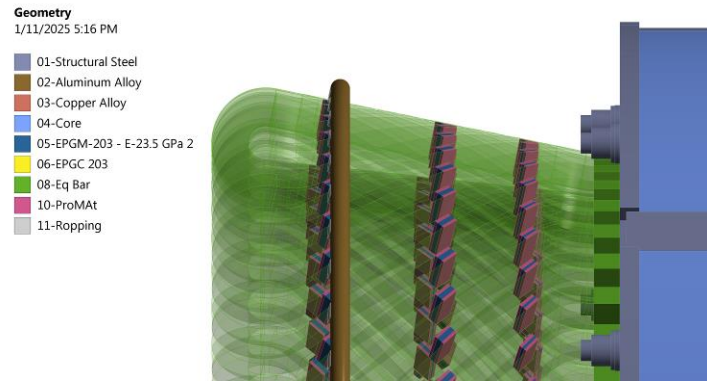


Figure 5. End-winding support system; Type D.

Table 5. The Type D Design Frequency Response

Ring Roping Young's Modulus (MPa)	With Ring		Without Ring
	E=120	E=200	
Mode Shape 4-Node (Hz)	177.65	184.91	158.86
Mode Shape 6-Node (Hz)	206.59	211.43	190.85
Mode Shape 8-Node (Hz)	243.5	248.27	229.5

5.5 The Type E design: The Type D design with an aluminium ring diameter of 25 mm

In the Type E design, the aluminum ring diameter is increased from 15 mm to 25 mm. Along with this increase, the ropping configuration must also be adjusted, as shown in Fig. 6.

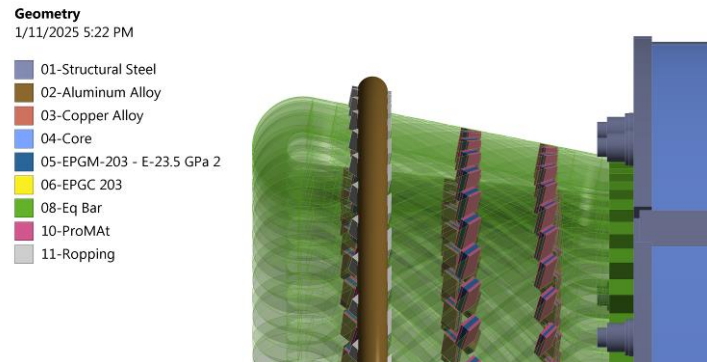


Figure 6. End-winding support system; Type E.

With the increased aluminium ring diameter, the eight-node natural frequency of the end coil increases by 17.7 Hz, reaching 265.96 Hz, demonstrating the positive impact of this change on the natural frequencies.

Table 6. The Type E Design Frequency Response

Ring Roping Young's Modulus (MPa)	With Ring		Without Ring
	E=120	E=200	
Mode Shape 4-Node (Hz)	188.22	193.87	158.86
Mode Shape 6-Node (Hz)	216.52	222.61	190.85
Mode Shape 8-Node (Hz)	259.54	265.96	229.5

The aluminium ring, previously modelled without insulation, was updated to include a 1 mm fiberglass insulation layer to replicate the real machine's configuration. This layer, with a Young's modulus of 500 MPa and density of 2600 kg/m³, was added to prevent magnetic flux formation. The frequency analysis showed only minor differences compared to the uninsulated case, indicating that the thin, resin-impregnated insulation has a negligible impact on the ring's performance and natural frequencies. The 6- and 8-Node mode shapes of the end-winding region of the DE sections of the medium-power motor can be seen in Fig. 7.

Table 7. The Type E Design Frequency Response with Insulation Layer

Ring Roping Young's Modulus (MPa)	With Ring	Without Ring
	E=200	
Mode Shape 4-Node (Hz)	194.01	158.86
Mode Shape 6-Node (Hz)	222.87	190.85
Mode Shape 8-Node (Hz)	266.23	229.5

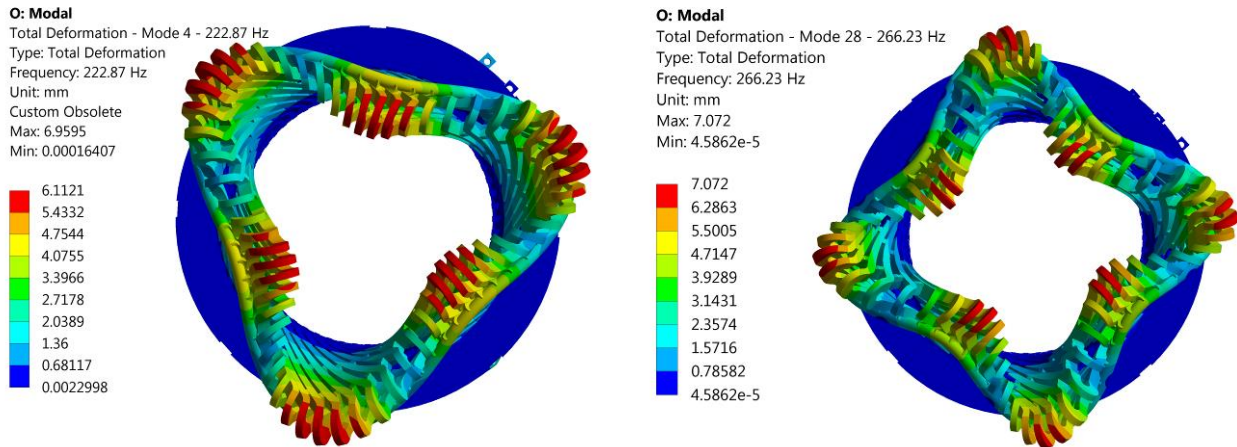


Figure 7. Modal analysis of end-winding Type E, a) 6-Node mode shape, b) 8-Node mode shape

5.6 Physical Interpretation and Sensitivity Discussion

Although the results are presented in terms of natural frequency variations, the observed trends can be explained by changes in the stiffness distribution of the end-winding supporting system. Increasing the number of roping rows enhances the circumferential stiffness of the structure, limiting the relative motion between adjacent coils. This effect is more pronounced for higher nodal diameter modes, particularly the eight-node mode, which exhibits greater sensitivity to circumferential stiffness.

The introduction of an aluminum annular ring further increases the global stiffness of the end-winding region by providing a continuous load path around the coil ends. The influence of the ring strongly depends on its axial position. When located closer to the coil bends, the ring more effectively constrains bending-dominated deformation patterns, leading to a more significant increase in natural frequencies. A qualitative sensitivity assessment indicates that the axial position of the supporting ring has a stronger influence on the eight-node natural frequency than the number of roping rows alone. These consistent trends across all design variants demonstrate a clear relationship between stiffness distribution and the modal behavior of the end-winding region.

6. Conclusion

This paper presented a frequency analysis of the end-windings in a medium-power, four-pole induction motor. The supporting system design was inspired by advanced practices adopted by leading manufacturers, aiming to achieve higher natural frequencies and enhanced vibration stability. Several design alternatives were evaluated, differing in the number of roping rows and the placement of the supporting ring.

Ultimately, the Type E design was identified as the most suitable configuration for the supporting system. The analysis showed that an aluminum annular ring, when properly roped around the coils, significantly increases system stiffness and elevates the natural frequencies. The placement of this ring was found to be a critical factor, with positioning closer to the coil bends yielding the most favorable results.

Acknowledgement

The authors would like to thank MAPNA Pars for its technical assistance and its authorization to publish this research.

REFERENCES

1. A. Merkhouf, B. F. Boueri, and H. Karmaker, *Generator end windings forces and natural frequency analysis*, 2003.
2. Y. Zhao, B. Yan, C. Chen, J. Deng, and Q. Zhou, "Parametric Study on Dynamic Characteristics of Turbogenerator Stator End Winding," *Energy Conversion, IEEE Transactions on*, vol. 29, pp. 129-137, 03/01 2014.
3. C. Kreischer, S. Kulig, and D. Thien, "Modal analysis of operational end winding vibrations," 05/01 2011.
4. J. Letal, M. Sasic, and J. Elyes, "Monitoring of Stator Endwinding Vibration on Motors and Generators," presented at the PCIC ME 2019, Vancouver, CanadaIEEE-PCIC, 2019.
5. P. G. S. Kumar, K. M. Reddy, and K. Kaylan Kumar, "Reinforcement of Generator Stator End Winding Structure by Modal Analysis Approach," presented at the 2019 IEEE 4th International Conference on Condition Assessment Techniques in Electrical Systems (CATCON), Chennai, India, 2019.
6. Y. Zhao, Y. Xiao, S. Lu, H. Sun, W. Huo, and Y. Liao, "Investigation on large turbo-generator stator end winding dynamic characteristics based on response surface method," *Journal of Power Electronics*, vol. 21, pp. 1473-1483, 2021.
7. M. Samadpour, A. Rezaei, and H. Kalantari, "250MVA Turbo-Generator end-winding vibration," presented at the 29th Annual International Conference of Iranian Association of Mechanical Engineers and 8th International Conference on Thermal Power Plants Industry, Tehran, 2021.
8. K. V Sri Ram Prasad and V. Singh, "Experimental modal analysis of induction machine stator end windings of driving end and non-driving end to predict the looseness," *Journal of Failure Analysis and Prevention*, vol. 22, pp. 1151-1163, 2022.
9. Z. Xing, X. Wang, and W. Zhao, "An Accurate Calculation Method of Natural Frequencies of the Radial-Flux Slotted Motors Considering End Covers," *IEEE Transactions on Industrial Electronics*, vol. 70, pp. 5516-5526, 2023.
10. B. Bahrami Joo, M. Dehghani, and M. Nikfar, "Multiphysics Analysis of the End winding Support System for a Medium Power Air-cooled Turbo-generator," presented at the 4th International Conference on Electrical Machines and Drives (ICEMD), Tehran, Iran, 2024.
11. M. Shahparasti, M. Dehghani, and M. Nikfar, "Frame and Stator Core Vibration Analysis of a Medium Power Generator through Finite Element Method," presented at the 2024 4th International Conference on Electrical Machines and Drives (ICEMD), Tehran, 2024.
12. Ranran Lin, Antti Nestori Laiho, Ari Haavisto, and Antero Arkkio, "End-Winding Vibrations Caused by Steady-State Magnetic Forces in an Induction Machine," *IEEE TRANSACTIONS ON MAGNETICS*, vol. 46, 2010.